Control of selectivity, activity and durability of simple supported nickel catalysts for hydrolytic hydrogenation of cellulose

Hirokazu Kobayashi,[a] Yuto Hosaka,[a,b] Kenji Hara,[a] Bo Feng,[a] Yoshihiko Hirosaki[a,b] and Atsushi Fukuoka*[a]

[a]Catalysis Research Centre, Hokkaido University, Kita 21 Nishi 10, Kita-ku, Sapporo, Hokkaido 001-0021, Japan

[b]Graduate School of Chemical Sciences and Engineering, Hokkaido University, Kita 13 Nishi 8, Kita-ku, Sapporo, Hokkaido 060-8628, Japan

*E-mail: fukuoka@cat.hokudai.ac.jp, Fax: +81 11 706 9139

Abstract

Efficient conversion of cellulose to sorbitol and mannitol by base metal catalysts is a challenge in green and sustainable chemistry, but typical supported base metal catalysts have not given good yields of hexitols or possessed durability. In this study, it has been demonstrated that a simple carbon-supported Ni catalyst affords up to 67% yield of hexitols in the conversion of cellulose, and that the catalyst is durable in the reuse experiments for 7 times. In addition, the catalyst can be separated by a magnet thanks to high content of Ni. Physicochemical analysis has indicated that the use of carbon supports has two benefits: no basicity and high water-tolerance. CeO_2, ZrO_2, γ-Al_2O_3 and TiO_2 cause side-reactions due to basicity, and SiO_2, γ-Al_2O_3 and CeO_2 are less stable in hot water. Another important factor is high Ni loading as increase of Ni content from 10 wt% to 70 wt% drastically improves yield of hexitols and durability of catalysts. Larger crystalline Ni particles are more resistant to sintering of Ni and surface coverage by Ni oxide species.

Introduction

Catalytic conversion of cellulose, an abundant and waste biomass, into chemicals and fuels is of

significant interest for nurturing sustainable societies.[1] Cellulose consists of glucose units linked by β-1,4-glycosidic bonds with inter- and intra-molecular hydrogen bonds, and thus cellulose can be hydrolysed to glucose and subsequently hydrogenated to sorbitol and mannitol (Scheme 1). These hexitols are precursors to engineering plastics such as polyisosorbide carbonate (PIC), plasticisers, environmentally-benign surfactants including Span and Tween, medicines and foods.[1b] However, industrial production of hexitols from cellulose has not yet been achieved, and these manufactures have been currently derived from starch, a food biomass.

In recent years, supported noble metal catalysts have been studied to convert cellulose into hexitols in one-pot.[2] Since noble metals are resourceless (production amounts: Pt, 211 t y^{-1} in 2006; Ru, 29 t y^{-1} in 2009) and expensive, development of base metal catalysts is a next challenge. Among the first-row transition metals, Ni (1,420,000 t y^{-1} in 2007) would be the most promising catalyst for this reaction as the hydrogenation of glucose to sorbitol has been practically performed with Raney Ni Catalyst.[1b] Indeed, supported nickel phosphides show good catalytic activity for the hydrolytic hydrogenation of cellulose, but these catalysts quickly deactivate because of the P leaching and Ni sintering.[3] A crystalline Ni metal on the tip of carbon fibres [Ni(3)/CNF; the loading amount (wt%) is shown in parenthesis hereafter] prepared by methane decomposition using Ni/γ-Al_2O_3 affords a good yield of hexitols as high as 56%, and the catalyst was durable in reuse experiments for three times.[4] The oxidation of this special catalyst by HNO_3 and subsequent impregnation of Ni(7.5) further raise the yield of hexitols up to 76%, due to the good rate balance between hydrolysis and hydrogenation.[5] In contrast, simple supported Ni metal catalysts [Ni(3)/C, Ni(16)/C, Ni(20)/C, Ni(3)/Al_2O_3, Ni(40)/Al_2O_3, Ni(40)/TiO_2, Ni(40)/SiO_2] have afforded low yields of hexitols less than 20%.[3,4,6,7] These results imply that the catalytic activity of Ni may be drastically affected by supports and loading state of Ni. Sels *et al.* and Zhao *et al.* independently proposed that one of the factors for good activity might be the large amount of (111) plane.[4,6] However, Ni (111) is the most stable and commonly appears, and thus this fact would not be a sole reason for the activity difference. It has been still unclear why usual supported Ni catalysts are inactive and some specific Ni catalysts are active. Besides, a mesoporous carbon-supported Ni(20) catalyst is also active for the conversion of

cellulose (hexitols 42% yield), but this catalyst is deactivated within three reuses.[7] So far, what controls the durability of Ni catalysts has not yet been studied. In this paper, we report fairly durable and active Ni catalysts prepared by a conventional impregnation method with a simple carbon support for the conversion of cellulose and discuss the distinction between active and inactive catalysts other than the effect of facet.

Experimental

Reagents

Microcrystalline cellulose (Avicel, 102331) was obtained from Merck and ball-milled with ZrO_2 balls (1 cm, 1 kg) in a ceramic bottle (900 mL) at 60 rpm for 4 days. This ball-milled cellulose was not soluble in water due to negligible mechanochemical hydrolysis under the mild milling conditions.[8] The content of physisorbed water in the cellulose was determined with total organic carbon measurement (TOC; Shimadzu, TOC-V CSN). Glucose, $Ni(NO_3)_2{\cdot}6H_2O$ (99.9%) and distilled water were purchased from Wako. Catalyst supports used in this study were as follows: carbon black KB (Lion, Ketjenblack EC-600JD, 1310 $m^2\ g^{-1}$), carbon black XC (Cabot, Vulcan XC72, 210 $m^2\ g^{-1}$), SiO_2 (Fuji silysia, CARiACT Q-6, 450 $m^2\ g^{-1}$), Al_2O_3 [Catalysis Society of Japan (CSJ), JRC-ALO-2, γ-Al_2O_3, 290 $m^2\ g^{-1}$], TiO_2 (CSJ, JRC-TIO-4, 52 $m^2\ g^{-1}$), ZrO_2 (CSJ, JRC-ZRO-2, 250 $m^2\ g^{-1}$) and CeO_2 (CSJ, JRC-CEO-2, 120 $m^2\ g^{-1}$).

Catalyst preparation

Ni(70)/KB catalyst, where the value in parenthesis shows Ni loading (wt%), was prepared by a typical impregnation method as follows: $Ni(NO_3)_2$ aq. (11.9 mmol) was dropped into a mixture of KB (0.30 g) and water (20 mL), and the mixture was evaporated and dried at 373 K. The resulting solid was treated with H_2 (30 mL min^{-1}) at 673 K for 2 h. Note that the solid was calcined under O_2 (30 mL min^{-1}) at 673 K for 2 h prior to the H_2-reduction when oxide supports were used. The prepared catalyst was exposed to air at room temperature for easy handling and subsequently used for catalytic reactions and analysis with X-ray diffraction (XRD; Rigaku, Miniflex, Cu Kα radiation),

transmission electron microscopy (TEM; JEOL, JEM-2100F, 200 kV), X-ray photoelectron spectroscopy (XPS; JEOL, JPC-9010MC) and temperature-programmed reduction (TPR; BEL, Belcat, 5 vol% H_2/Ar).

Hydrolytic hydrogenation of cellulose

The conversion of ball-milled cellulose was conducted in a stainless steel (SUS316) high-pressure reactor (OM Lab-Tech, MMJ-100, 100 mL). Ball-milled cellulose [324 mg (containing 4–8 wt% physisorbed water)], catalyst (50 mg), and water (40 mL) were charged in the reactor, and then it was pressurised with H_2 of 5.0 MPa at 298 K. We chose this substrate/catalyst ratio (6.5 wt/wt) based on control experiments (Table S1). The mixture was heated to 483 K with stirring at 600 rpm and kept at that temperature for 6 h. Products were separated by centrifugation and decantation, and water-soluble products were analysed with a high-performance liquid chromatography (HPLC; Shimadzu LC10-AT*VP*, refractive index detector). Columns used in this work were a Phenomenex Rezex RPM-Monosaccharide Pb++ column (ø7.8×300 mm, mobile phase: water 0.6 mL min^{-1}, 343 K) and a Shodex Sugar SH-1011 column (ø8×300 mm, mobile phase: water 0.5 mL min^{-1}, 323 K). A by-product, hexanetetrol, was identified by ^{1}H nuclear magnetic resonance (NMR; JEOL ECX-400, 400 MHz) and liquid chromatography/mass spectrometry (LC/MS; JEOL JMS-T50LC AccuTOF, atmospheric pressure chemical ionisation) (see text and Fig. S1 in ESI†). Conversion of cellulose was determined from the difference of dry weight of solid before and after the reaction.

Results and discussion

Influences of Ni supports for hydrolytic hydrogenation

Reaction of ball-milled cellulose under H_2 pressure afforded 93% conversion without catalyst, which was mainly ascribed to the hydrolysis of cellulose by direct attack of water[9] and acidic by-products (Table 1, entry 1). No hexitols were obtained as a catalyst was essential for the reduction step. Nor was glucose, since glucose has a thermally-unstable aldehyde group in its linear structure and readily decomposes at the high temperature. In fact, 89% of glucose was degraded under aqueous conditions

without catalysts even at a lower temperature (463 K) for 3 h.[10] As a result, large quantities of by-products such as 5-hydroxymethylfurfural (5.9% yield) and humins (< 7%) were produced in this non-catalytic reaction.

Thus, Ni catalysts supported on carbons and metal oxides were tested in the hydrolytic hydrogenation of ball-milled cellulose. Ni(50)/KB catalyst gave 64% yield of hexitols (sorbitol 57% and mannitol 6.8%) with 71% selectivity based on the conversion of cellulose (90%) (entry 6). This catalytic performance was better than that of a commercial Raney Ni (hexitol yield: 40%, entry 15). Other products were sorbitan (2.4%), cellobitol (0.5%), hexanetetrol (5.4%), erythritol (1.3%), propylene glycol (PG; 1.7%), ethylene glycol (EG; 0.8%), glucose (0.2%) and unidentified compounds (15%). Ni-loaded SiO_2, Al_2O_3, TiO_2 and ZrO_2 provided lower yields of hexitols (28–43%), and Ni(50)/CeO_2 was almost inactive (entries 10–14). The less active for the production of hexitols the catalyst was, the higher yields of PG and EG the catalyst gave. Ni(50)/CeO_2 produced the largest amounts of PG and EG (total 26 %). Since hexitols are formed *via* the hydrolysis of cellulose to soluble glucans and the successive hydrogenation,[2f] the formation of PG and EG indicates base-catalysed retro-aldol reactions of the sugar intermediates (Scheme 2).[11] Furthermore, it is known that bases enhance the formal hydrogenolysis of sugar alcohols.[12] Thus, the yields of the C_2–C_3 polyols and those of hexitols afforded by supported Ni catalysts were plotted against the electonegativities of respective support metals (Fig. 1), as the basicity of metal oxides correlates with this parameter.[13] Fig. 1 illustrates that more negative metal results in a higher yields of hexitols and less yields of the C_2–C_3 polyols. The position of C should be formally the right tip on the horizontal-axis because C virtually has no basicity, which agrees with the tendency in our reaction results. This good correlation indicates that basic supports promote the cleavage of C–C bonds to decrease the yield of hexitols.

Another considerable factor is the nature of Ni metal and degradation of supports during reactions. XRD measurements of supported Ni catalysts before and after the reaction provided peaks from Ni, oxidised Ni and supports (Fig. 2), and we focused on Ni peaks at first. The diffraction lines of Ni metal appeared at 2θ = 43° and 52° for all the Ni catalysts before reaction (Fig. 2a), and the crystallite diameters of Ni determined by the Scherrer equation were 20–30 nm except for

Ni(50)/KB (11 nm). However, the sizes of Ni crystallites turned into the same range (20-30 nm) during the reaction (Fig. 2b). We checked that another carbon-supported Ni catalyst Ni(50)/XC, in which Ni diameter was 20 nm, gave a similar yield of hexitols (57%, Table 1, entry 7) to that given by Ni(50)/KB (64%, entry 5). Accordingly, the particle size effect can be excluded in these particular cases.

Small broad peaks were observed at 37° for Ni(50)/KB and Ni(50)/SiO_2 (Fig. 2a), and these peaks were assigned to NiO (size: 2 nm). Ni metal particles are decorated with NiO as the catalysts have been exposed to air. Although other Ni catalysts may also have NiO, the peaks were not seen due to the low intensity and overlapped with diffraction lines of supports. New broad and weak peaks were observed at 34° for KB, SiO_2, Al_2O_3, TiO_2 and CeO_2-supported Ni catalysts after reactions (Fig. 2b), which indicated the formation of $Ni(OH)_2$ by the hydration of NiO. This peak could not be observed for Ni(50)/ZrO_2 owing to overlap with those from ZrO_2. Hence, we tentatively conclude that all the catalysts have oxidised Ni species similarly on the surface. Effect of these oxidised species is discussed in the next section.

The XRD patterns of supports were compared before and after the reactions. KB provided a very small and broad peak attributed to amorphous carbon at 24°, and this peak did not change after the reaction. Although carbon has another broad peak at 43°, it is invisible in this case due to the overlap with a large peak of Ni. It is well known that carbon is highly stable in hot water. SiO_2 also retained amorphous nature in the reaction, and a new peak at 22° after the reaction was attributed to cellulose IV crystals formed during the reaction. However, SiO_2 slightly dissolves in water especially at high temperatures,[14] and hence the lower activity of non-basic Ni/SiO_2 than Ni/KB might be due to the degradation of SiO_2 under the reaction conditions. Likewise, γ-Al_2O_3 (36, 39°) turned into boehmite [AlO(OH)] (28, 39, 49°), and the low durability of γ-Al_2O_3-supported catalysts was demonstrated in the hydrolytic hydrogenation of cellulose in previous studies.[2f,15] TiO_2 kept the mixed structure of rutile (major diffraction line: 27°) and anatase (25°), and ZrO_2 maintained that of tetragonal zirconia (30°) and monoclinic zirconia (28°, 32°). These supports are fairly stable in hot water. Fluorite structure of CeO_2 (28°, 33°, 47°, 56°) was also transformed into unidentified one (25°, 31°, 43°, 47°),

which is probably assignable to hydrated or partially reduced species.

Consequently, the carbon support affords high yields of hexitols thanks to no basicity and high stability under the reaction conditions.

Hydrolytic hydrogenation of cellulose by Ni/KB catalyst

The hydrolytic hydrogenation of ball-milled cellulose was conducted using Ni/KB catalysts with varied Ni loading of 0–70 wt%. Although Ni-free KB degraded cellulose in 85% conversion, hexitols were not produced as Ni was essential for the hydrogenation step (Table 1, entry 2). Ni(10)/KB only gave 5.2% yield of hexitols, but the yield was dramatically improved to 28%, 49% and 64% with increasing the loading amount of Ni to 30, 40 and 50 wt%, respectively (entries 3–6). Ni(70)/KB afforded a similar yield of hexitols (59%) to that obtained by Ni(50)/KB (entry 7). The hydrogenation rate might strongly depend on the Ni loading, which determines the yield of hexitols. If the hydrogenation is slow, glucose easily undergoes decomposition as described above. Meanwhile, it is notable that a catalyst containing $\geq$50 wt% Ni can be recovered using a magnet (Fig. S2, ESI†). We have also checked that microcrystalline cellulose can be converted to hexitols by Ni(70)/KB (entry 8), although the yield (21%) is lower than that in the reaction of ball-milled cellulose (59%) due to higher crystallinity (Crystallinity Index for microcrystalline cellulose: 81%, for ball-milled cellulose: 14%).

The hydrogenation activities of Ni(10–70)/KB catalysts were measured in the reduction of glucose at 373 K under 5 MPa of H_2 (Table 2). Hydrogenation rates of the Ni catalysts were in a narrow range of 230 to 390 μmol h^{-1} (entries 16–19); however, they were drastically decreased after treating in water at 483 K for 2 h under 5 MPa of H_2 (entries 20–23). Ni(10)/KB and Ni(30)/KB became completely inactive for the hydrogenation of glucose, whereas Ni(50) and Ni(70) catalysts partially maintained the activities (57 and 62 μmol h^{-1}, respectively). Hence, these reduced activities correlate with the large difference of the yields of hexitols in the cellulose conversion by the Ni(10–70)/KB catalysts (Table 1, entries 3–7), although small amounts of hexitols are produced by Ni(10) and Ni(30) catalysts before the deactivation.

We measured XRD patterns of Ni/KB catalysts to clarify the cause of deactivation. Pristine Ni/KB catalysts provided diffraction lines of Ni metal at 43° (Fig. 3a), and the crystallite diameters of Ni were 2.7, 4.3, 11 and 16 nm for Ni(10), Ni(30), Ni(50) and Ni(70)/KB catalysts, respectively. These four catalysts also showed broad weak peaks of NiO at 37°, of which the size was 2 nm in all cases. XPS and TPR studies were conducted to quantify the oxidised Ni species using the lowest and highest Ni loading catalysts: Ni(10)/KB and Ni(70)/KB. Both catalysts provided peaks of NiO (854.1 eV) with satellite peaks (861 eV) and Ni metal (852.6 eV) in Ni $3p_{3/2}$ XPS analysis (Fig. 4).[16] The ratio of $Ni^0/(Ni^0+Ni^{II})$ at near surface was 14% for Ni(10)/KB and 28% for Ni(70)/KB. TPR measurements indicated that the fraction of bulk Ni^0 was 29% for Ni(10)/KB and 85% for Ni(70)/KB (Fig. S3), thus showing that Ni(10)/KB was significantly more oxidised than Ni(70)/KB. Moreover, the lower ratios of Ni metal at near surfaces than those in bulk phases suggest that the surface of Ni particles is oxidised. TEM observation of Ni(50)/KB exhibited spherical Ni particles (Fig. 5), and the average particle diameter (d_{av}) defined to keep the surface area of original particles (eqn. 1, see ESI†) was 14 nm for Ni(50)/KB. This value is similar to the XRD data (11 nm), and becomes almost the same by subtracting the thickness of NiO [2 nm (one side of Ni) to 4 nm (both side)] from 14 nm. Note that the shape of Ni was homothetic without dependence of the loading amount (Fig. S4, ESI†). Thus, XRD is useful to estimate the number of surface Ni atoms, excluding the oxide. NiO could not be identified by TEM observation due to its limited resolution. The turnover frequencies (TOFs) for the hydrogenation of glucose per number of surface Ni are 9.7, 6.5, 9.7 and 7.7 h^{-1} for pristine Ni(10), Ni(30), Ni(50) and Ni(70) catalysts, respectively (Table 2, entries 16–19). Accordingly, the hydrogenation activity of surface Ni atom is independent of the particle size or Ni loading for the non-treated catalysts. The particle sizes of Ni after the treatment in water at 483 K were 28, 26, 28 and 21 nm for Ni(10), Ni(30), Ni(50) and Ni(70)/KB catalysts, respectively (Fig. 3b). Lower Ni loading catalysts caused more severe sintering as small Ni particles easily aggregate. In addition, oxidised Ni dissolves at the reaction temperature and deposits again, which is a typical sintering mechanism in liquid phase. In fact, small broad diffraction lines of $Ni(OH)_2$ were observed at 34° for all the catalysts after the treatment. This effect of oxide species would be serious

for Ni(10) and Ni(30) catalysts as the fractions of NiO are higher than those in Ni(50) and Ni(70) catalysts as described above. Indeed, XPS analysis revealed that Ni(10)/KB had $Ni(OH)_2$ (856.0 eV)[16] without Ni metal near the surface, whereas Ni(70)/KB had a 22% fraction of Ni metal (Fig. 4). TOFs for respective catalysts were 0.0, 0.0, 3.7 and 2.2 h^{-1} (entries 20–23), and hence the catalytic activities after the treatment did not well correlate with the theoretical number of surface Ni atoms. Therefore, we tried to reduce the deactivated Ni(10)/KB catalyst under H_2 flow at 673 K, by which the weak peak of $Ni(OH)_2$ at 34° disappeared and the intensity of Ni increased (Fig. 6). This reduced catalyst afforded a high TOF of 31 h^{-1} for the hydrogenation of glucose (entry 24). The complete deactivation of Ni(10) and Ni(30)/KB catalysts is ascribed to the surface coverage by oxidised Ni species mainly composed of $Ni(OH)_2$ (Fig. S5, ESI†).

$$\text{Average diameter } (d_{av}) = \sum_k d_k^3 \Big/ \sum_k d_k^2 \quad (1)$$

, where d_k is diameter of kth Ni particle.

Our results imply that a higher Ni loading catalyst shows better durability, because the catalyst is more resistant to sintering and has a lower fraction of oxide species. This hypothesis motivated us to compare the durability of Ni(50)/KB and Ni(70)/KB catalysts in the hydrolytic hydrogenation of ball-milled cellulose. The solid residue containing catalyst and unreacted cellulose was used for the next reaction by adding fresh ball-milled cellulose of 1620 mg. The remaining cellulose in the previous run has a negligible effect in the subsequent run because the conversion of cellulose is as high as 90% in these experiments. Ni(70)/KB gave hexitols in 56–67% yields in the repeated runs for 7 times [Fig. 7(a)]. Total turnover numbers (TONs) based on initial surface and bulk Ni atoms were 218 and 14, respectively, thus showing that Ni clearly worked as a catalyst. Ni(70)/KB catalyst was fairly durable, but the yields decreased to 49% (8th run) and 42% (9th). Particle diameter of Ni on the catalyst was 26 nm after the 9th run. Since the diameter of Ni was already 21 nm after the treatment for 2 h as mentioned in the previous paragraph, the sintering of Ni was limited in the repeated reactions. Ni of 35 ppm, corresponding to 0.45% of the catalyst, leached out into the

reaction solution in each run, and thus 96% of Ni remained on the catalyst after the 9th run. The major cause of deactivation would be oxidation of Ni as indicated in the model reactions using glucose. On the other hand, Ni(50)/KB deactivated in the 3rd run; the yields of hexitols were 59% (1st), 53% (2nd) and 35% (3rd) [Fig. 7(b)]. Higher Ni loading is the key to the better durability in the conversion of cellulose. From that viewpoint, it is noteworthy that Ni(3)/CNF is durable for 3 times regardless of the low loading amount.[4] We speculate that the special features of this catalyst, namely, large crystal size of Ni (*ca.* 100 nm) and fixation of Ni on the rigid carbon frame may avoid sintering and coverage by oxides.

Conclusion

We have demonstrated that a simple carbon-supported Ni catalyst, Ni(70)/KB, is active for the production of hexitols from cellulose, and that the catalyst is fairly durable. In addition, the catalyst can be separated by a magnet thanks to the high content of Ni. The use of carbon supports has two benefits: no basicity and high water-tolerance. CeO_2, ZrO_2, γ-Al_2O_3 and TiO_2 have basicity causing side-reactions, and SiO_2, γ-Al_2O_3 and CeO_2 are less stable in hot water. Another important factor is the high loading amount of Ni as the increase of Ni content from 10 wt% to 70 wt% drastically improves the yield of hexitols and durability. Larger crystalline Ni particles are more resistant to sintering and the surface coverage by Ni oxide species. These findings would help understanding of the performance of various Ni catalysts in the hydrolytic hydrogenation and also be useful to design more active and durable Ni catalysts for the conversion of cellulose.

Acknowledgment

This work was supported by a Grant-in-Aid Scientific Research (KAKENHI, 20226016) from Japan Society for the Promotion of Science (JSPS).

References

1 (*a*) C. O. Tuck, E. Pérez, I. T. Horváth, R. A. Sheldon and M. Poliakoff, *Science*, 2012, **337**,

695-699; (*b*) H. Kobayashi and A. Fukuoka, *Green Chem.*, 2013, **15**, 1740-1763; (*c*) A. Brandt, J. Gräsvik, J. P. Hallett and T. Welton, *Green Chem.*, 2013, **15**, 550-583; (*d*) P. Gallezot, *Chem. Soc. Rev.*, 2012, **41**, 1538-1558; (*e*) W. Deng, Y. Wang, Q. Zhang and Y. Wang, *Catal. Surv. Asia*, 2012, **16**, 91-105; (*f*) S. Van de Vyver, J. Geboers, P. A. Jacobs and B. F. Sels, *ChemCatChem*, 2011, **3**, 82-94; (*g*) C.-H. Zhou, X. Xia, C.-X. Lin, D.-S. Tong and J. Beltramini, *Chem. Soc. Rev.*, 2011, **40**, 5588-5617; (*h*) M. J. Climent, A. Corma and S. Iborra, *Green Chem.*, 2011, **13**, 520-540; (*i*) J. J. Verendel, T. L. Church and P. G. Andersson, *Synthesis*, 2011, **11**, 1649-1677; (*j*) D. M. Alonso, J. Q. Bond and J. A. Dumesic, *Green Chem.*, 2010, **12**, 1493-1513.

2 (*a*) A. Fukuoka and P. L. Dhepe, *Angew. Chem. Int. Ed*., 2006, **45**, 5161-1563; (*b*) C. Luo, S. Wang and H. Liu, *Angew. Chem. Int. Ed.*, 2007, **46**, 7636-7639; (*c*) W. Deng, X. Tan, W. Fang, Q. Zhang and Y. Wang, *Catal. Lett.*, 2009, **133**, 167-174; (*d*) J. Geboers, S. Van de Vyver, K. Carpentier, K. de Blochouse, P. Jacobs and B. Sels, *Chem. Commun.*, 2010, **46**, 3577-3579; (*e*) R. Palkovits, K. Tajvidi, A. M. Ruppert and J. Procelewska, *Chem. Commun.*, 2011, **47**, 576-578; (*f*) H. Kobayashi, Y. Ito, T. Komanoya, Y. Hosaka, P. L. Dhepe, K. Kasai, K. Hara and A. Fukuoka, *Green Chem.*, 2011, **13**, 326-333; (*g*) H. Kobayashi, H. Matsuhashi, T. Komanoya, K. Hara and A. Fukuoka, *Chem. Commun.*, 2011, **47**, 2366-2368; (*h*) J. Geboers, S. Van de Vyver, K. Carpentier, P. Jacobs and B. Sels, *Green Chem.*, 2011, **13**, 2167-2174; (*i*) M. Liu, W. Deng, Q. Zhang, Y. Wang and Y. Wang, *Chem. Commun.*, 2011, **47**, 9717-9179; (*j*) J. W. Han and H. Lee, *Catal. Commun.*, 2012, **19**, 115-118; (*k*) D. Reyes-Luyanda, J. Flores-Cruz, P. J. Morales-Pérez, L. G. Encarnación-Gómez, F. Shi, P. M. Voyles and N. Cardona-Martínez, *Top. Catal.*, 2012, **55**, 148-161; (*l*) J. Hilgert, N. Meine, R. Rinaldi and F. Schüth, *Energy Environ. Sci.*, 2013, **6**, 92-96; (*m*) T. Deng and H. Liu, *Green Chem.*, 2013, **15**, 116-124.

3 L.-N. Ding, A.-Q. Wang, M.-Y. Zheng and T. Zhang, *ChemSusChem*, 2010, **3**, 818-821; P. Yang, H. Kobayashi, K. Hara and A. Fukuoka, *ChemSusChem*, 2012, **5**, 920-926.

4 S. Van de Vyver, J. Geboers, M. Dusselier, H. Schepers, T. Vosch, L. Zhang, G. Van Tendeloo, P. A. Jacobs and B. F. Sels, *ChemSusChem*, 2010, **3**, 698-701.

5 S. Van de Vyver, J. Geboers, W. Schutyser, M. Dusselier, P. Eloy, E. Dornez, J. W. Seo, C. M.

Courtin, E. M. Gaigneaux, P. A. Jacobs and B. F. Sels, *ChemSusChem*, 2012, **5**, 1549-1558.

6 G. Liang, H. Cheng, W. Li, L. He, Y. Yu and F. Zhao, *Green Chem.*, 2012, **14**, 2146-2149.

7 J. Pang, A. Wang, M. Zheng, Y. Zhang, Y. Huang, X. Chen and T. Zhang, *Green Chem.*, 2012, **14**, 614-617.

8 H. Kobayashi, M. Yabushita, T. Komanoya, K. Hara, I. Fujita and A. Fukuoka, *ACS Catal.*, 2013, **3**, 581-587.

9 O. Bobleter, *Prog. Polym. Sci.*, 1994, **19**, 797-841.

10 H. Kobayashi, H. Ohta and A. Fukuoka, *Catal. Sci. Technol.*, 2012, **2**, 869-883.

11 D. Esposito and M. Antonietti, *ChemSusChem*, 2013, **6**, 989-992.

12 I. T. Clark, *Ind. Eng. Chem.*, 1958, **50**, 1125-1126; J. Sun and H. Liu, *Green Chem.*, 2011, **13**, 135-142.

13 K. Shimizu, K. Sawabe and A. Satsuma, *Catal. Sci. Technol.*, 2011, **1**, 331-341; K. Shimura and K. Shimizu, *Green Chem.*, 2012, **14**, 2983-2985.

14 G. B. Alexander, W. M. Heston and R. K. Iler, *J. Phys. Chem.*, 1954, **58**, 453-455.

15 R. M. Ravenelle, J. R. Copeland, W.-G. Kim, J. C. Crittenden and C. Sievers, *ACS Catal.*, 2011, **1**, 552-561; R. M. Ravenelle, J. R. Copeland, A. H. Van Pelt, J. C. Crittenden and C. Sievers, *Top. Catal.*, 2012, **55**, 162-174.

16 C. D. Wanger, W. M. Riggs, L. E. Davis, J. F. Moulder and G. E. Muilenberg, *Handbook of X-Ray Photoelectron Spectroscopy*, Perkin-Elmer Corporation, Eden Prairie, 1979; H. W. Nesbitt, D. Legrand and G. M. Bancroft, *Phys. Chem. Minerals*, 2000, **27**, 357-366.

Tables

Table 1 Hydrolytic hydrogenation of cellulose by Ni catalysts[a]

Entry	Catalyst	Conv. /%	Yield /%C										
			Hexitols			Sorbitan	Cellobitol	HT[b]	ET[c]	PG[d]	EG[e]	Glucose	Others[f]
			Sorbitol	Mannitol	Total								
1	None	93	0	0	0	0	0	0	0	0	0	0.5	92
2	KB	85	0	0	0	0	0	0	0	0	0	0.9	84
3	Ni(10)/KB	86	3.8	1.4	5.2	0	0	2.8	0.4	1.5	1.3	1.1	74
4	Ni(30)/KB	86	24	3.7	28	1.0	0	4.2	1.2	3.2	1.9	0.7	46
5	Ni(40)/KB	89	43	5.7	49	1.6	0	5.2	1.4	1.8	1.6	0.4	28
6	Ni(50)/KB	90	57	6.8	64	2.4	0.5	5.4	1.3	1.7	0.8	0.2	14
7	Ni(70)/KB	87	52	7.3	59	3.3	0.6	6.3	1.3	1.7	0.9	0.2	14
8[g]	Ni(70)/KB	42	18	3.2	21	0.5	0.7	4.3	0.6	1.4	0.7	0.2	12
9	Ni(50)/XC	91	52	5.3	57	1.8	0.6	7.6	1.6	1.5	0.9	0.2	20
10	Ni(50)/SiO_2	92	37	6.0	43	2.6	0.7	8.4	1.4	2.1	1.2	0	33
11	Ni(50)/Al_2O_3	87	26	3.6	30	1.5	0.8	8.7	2.2	4.6	2.8	0.6	36
12	Ni(50)/TiO_2	85	36	5.6	41	3.2	0.4	9.0	1.7	3.8	1.8	0.1	24
13	Ni(50)/ZrO_2	88	23	4.6	28	2.2	0.4	9.4	1.9	5.9	3.3	0.2	37
14	Ni(50)/CeO_2	65	1.3	0.7	2.0	0.5	0	2.3	1.0	8.9	17	1.1	32
15	Raney Ni	86	31	9.2	40	0	1.9	8.7	0.9	3.0	2.1	0	29

[a] Reaction conditions; ball-milled cellulose 324 mg (containing physisorbed water 4–8 wt%), catalyst 50 mg, water 40 mL, reaction time 6 h, T = 483 K, $p(H_2)$ = 5.0 MPa at r.t. [b] Hexanetetrol. [c] Erythritol. [d] Propylene glycol. [e] Ethylene glycol. [f] Difference of the conversion and total yield of the identified products. [g] Microcrystalline cellulose (324 mg) was used as a substrate.

Table 2 Hydrogenation of glucose over Ni/KB catalysts[a]

Entry	Ni loading /wt%	Particle size[b] /nm	Surface Ni /μmol	Formation rate of sorbitol /μmol h^{-1}	TOF[c] /h^{-1}
16	10	3.6	24	230	9.7
17	30	4.3	60	390	6.5
18	50	11	39	380	9.7
19	70	16	38	290	7.7
20[d]	10	28	3.1	0	0
21[d]	30	26	9.9	0	0
22[d]	50	28	15	57	3.7
23[d]	70	21	29	62	2.2
24[d,e]	10	31	2.8	85	31

[a] Reaction conditions; glucose 90 mg (500 μmol), Ni/KB 50 mg, water 40 mL, reaction time 0.33 h, T = 373 K, $p(H_2)$ = 5.0 MPa at r.t. [b] Determined by XRD. [c] Turnover frequency based on the amount of surface Ni atoms and formation rate of sorbitol. [d] Catalyst was treated in water at 483 K for 2 h under H_2 of 5 MPa. [e] Catalyst was treated under H_2 flow (0.1 MPa) at 673 K for 2 h.

Scheme and fig. captions

Scheme 1 Conversion of cellulose to hexitols.

Scheme 2 Side-reactions of sugar compounds.

Fig. 1 Yields of hexitols and C_2–C_3 polyols as a function of electronegativity of support metal. Circle (●), total yield of sorbitol and mannitol; triangle (▲), total yield of PG and EG.

Fig. 2 XRD patterns of supported Ni catalysts (a) before and (b) after the hydrolytic hydrogenation of cellulose at 483 K for 6 h. Intensities at 20°–40° are 15 times enlarged. [a] 2 h, without cellulose. [b] 463 K, 16 h.

Fig. 3 XRD patterns of Ni/KB catalysts (a) before and (b) after the treatment in water at 483 K for 2 h under 5 MPa of H_2. Intensities at 20°–40° are 10 times enlarged.

Fig. 4 Ni $2p_{3/2}$ XP spectra of (a) Ni(10)/KB and (b) Ni(70)/KB before and after the treatment in water at 483 K under 5 MPa of H_2 for 2 h.

Fig. 5 TEM image of Ni(50)/KB catalyst.

Fig. 6 XRD patterns of treated Ni(10)/KB catalysts. Intensities at 20°–40° are 10 times enlarged.

Fig. 7 Reuse experiments of (a) Ni(70)/KB and (b) Ni(50)/KB in hydrolytic hydrogenation of cellulose. Catalyst, 250 mg; ball-milled cellulose, 1620 mg; water, 40 mL; $p(H_2)$, 5 MPa; 483 K; 6 h.

Schemes and Figs.

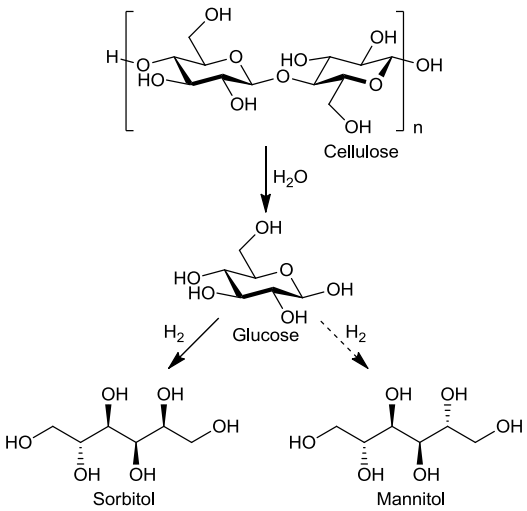

Scheme 1 Conversion of cellulose to hexitols.

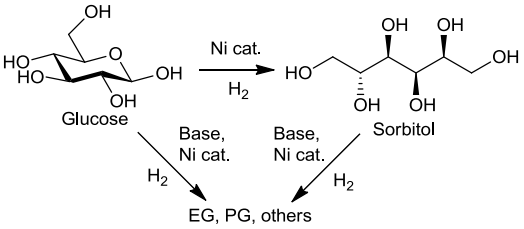

Scheme 2 Side-reactions of sugar compounds.

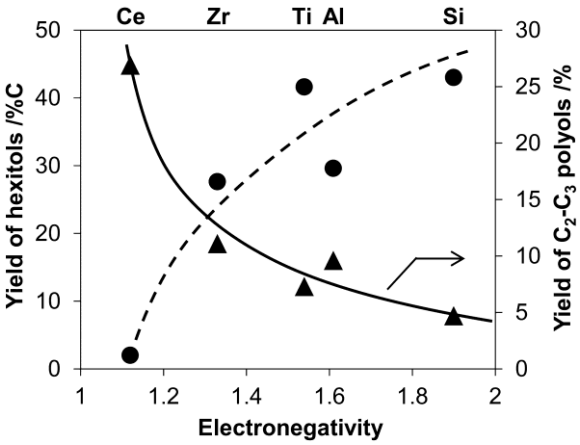

Fig. 1 Yields of hexitols and C_2–C_3 polyols as a function of electronegativity of support metal.

Circle (●), total yield of sorbitol and mannitol; triangle (▲), total yield of PG and EG.

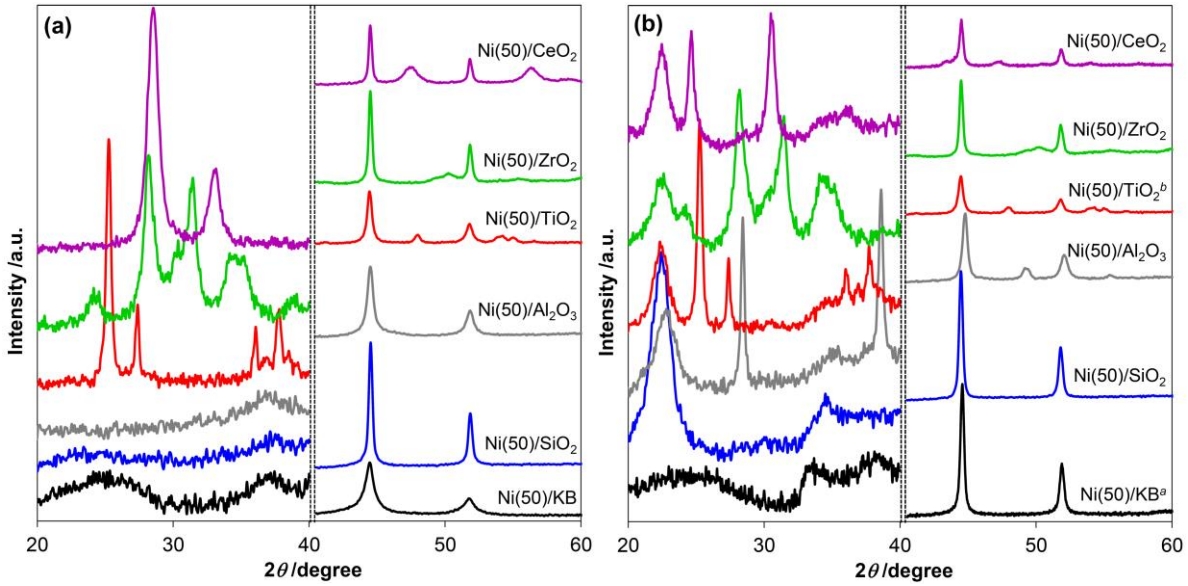

Fig. 2 XRD patterns of supported Ni catalysts (a) before and (b) after the hydrolytic hydrogenation of cellulose at 483 K for 6 h. Intensities at 20°–40° are 15 times enlarged. [a] 2 h, without cellulose. [b] 463 K, 16 h.

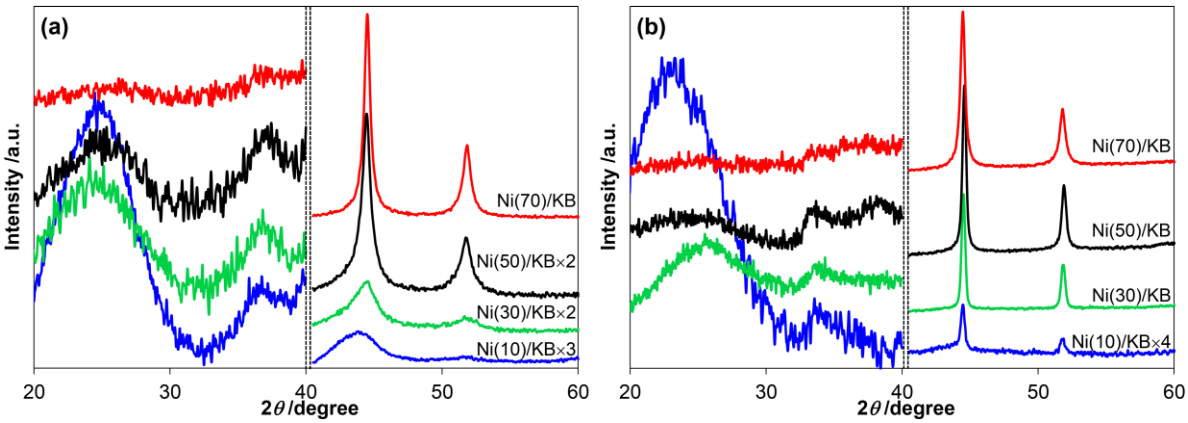

Fig. 3 XRD patterns of Ni/KB catalysts (a) before and (b) after the treatment in water at 483 K for 2 h under 5 MPa of H_2. Intensities at 20°–40° are 10 times enlarged.

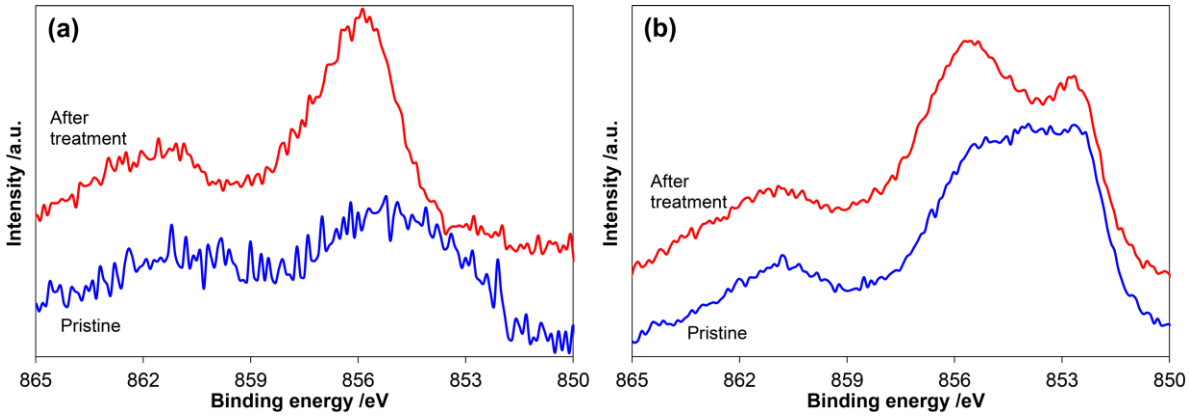

Fig. 4 Ni $2p_{3/2}$ XP spectra of (a) Ni(10)/KB and (b) Ni(70)/KB before and after the treatment in water at 483 K under 5 MPa of H_2 for 2 h.

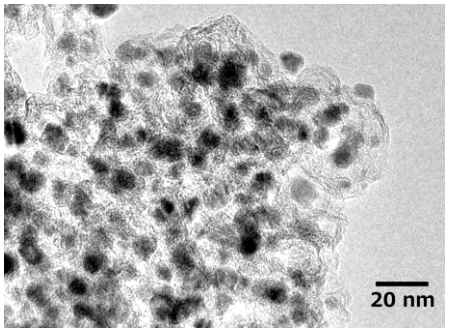

Fig. 5 TEM image of Ni(50)/KB catalyst.

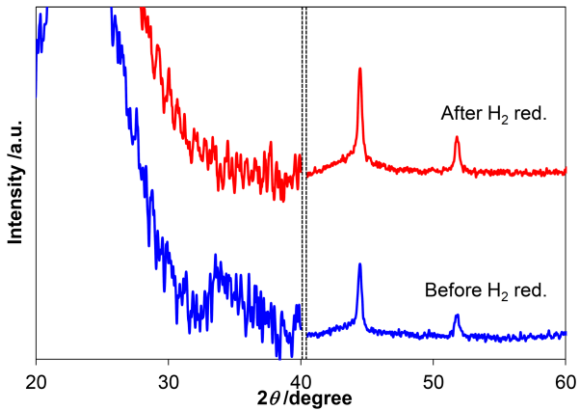

Fig. 6 XRD patterns of treated Ni(10)/KB catalysts. Intensities at 20°–40° are 10 times enlarged.

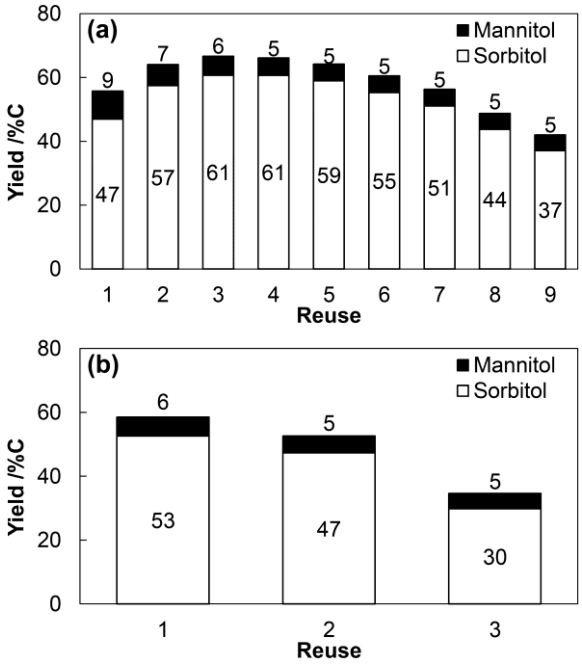

Fig. 7 Reuse experiments of (a) Ni(70)/KB and (b) Ni(50)/KB in hydrolytic hydrogenation of cellulose. Catalyst, 250 mg; ball-milled cellulose, 1620 mg; water, 40 mL; $p(H_2)$, 5 MPa; 483 K; 6 h.